POAC'23
Glasgow, United Kingdom

Proceedings of the 27th International Conference on
Port and Ocean Engineering under Arctic Conditions
12-16 June 2023, Glasgow, United Kingdom

Comparisons of mechanical properties between dry and floating saline ice

Mingdong Wei[1], Malith Prasanna[1], David M. Cole[2], Arttu Polojärvi[1]
[1] Aalto University, School of Engineering, Department of Mechanical Engineering, Espoo, Finland
[2] ERDC-CRREL (Ret.), 72 Lyme Rd., Hanover, NH 03768, USA

ABSTRACT

Experimental characterization of saline ice behavior is the basis of sea ice modeling. In many previous laboratory experiments, relatively cold, isothermal and dry ice specimens have been used instead of warm specimens or specimens floating in water. Even for the case of field experiments, sea ice specimens are often taken out of the seawater for testing. Therefore, the sea ice is often not tested under its natural conditions. Whether the dry and isothermal saline ice specimens behave similarly to floating specimens with the same average temperature, but with a naturally occurring temperature gradient, has been lacking assessment. In this study, uniaxial cyclic compression tests were carried out on laboratory-prepared saline ice under both dry and floating conditions. Our dry saline specimens showed ≈21% higher average elastic modulus than the corresponding floating specimens, although their average temperatures, salinities, bulk densities and porosities were approximately constant. Moreover, the floating specimens present much more pronounced rheological behavior than the dry specimens. Thus, our preliminary results indicate that the mechanical properties of dry and floating saline ice differ significantly.

KEY WORDS: Floating ice; Cyclic loading; Modulus; Rheological behavior; Flexural strength.

INTRODUCTION

The extent of sea ice has fallen in recent decades. The changes in ice-covered seas affect nearby ecosystems, ocean and atmospheric circulation, as well as global climate. Further, this reduced sea ice extent has increased human activities in polar regions, increasing the number of events where ice interacts with engineering structures, such as vessels, offshore wind turbines, and harbor facilities. For these reasons a comprehensive understanding of the physical and mechanical properties of sea ice is required—even large-scale climate models applied to polar regions need to incorporate the physical behavior of sea ice on them reliably (Feltham, 2008).

Sea ice must often sustain cyclic loading from waves. The interaction between sea ice and waves is highly complex and, for instance, under wave-induced cyclic loading, sea ice may suffer failure due to fatigue or even be strengthened in its mechanical properties (Iliescu et al., 2017; Murdza et al., 2020a, b, 2021). The interaction between sea ice and waves has led to recent extensive interests on the sea ice behavior under cyclic loading, motivating related in-situ and laboratory experiments and numerical simulations (Langhorne et al., 1998; Murdza et al., 2022; Squire, 2020).

Although in-situ testing is the most direct way to understand sea ice behavior, it often poses challenges and is costly. Consequently, laboratory testing has become a common approach to sea ice research. Small-scale laboratory experiments are still essential for understanding sea ice behavior. For such tests saline ice samples are often stored at some given temperature and for an arbitrary period of time before testing. The properties of such ice specimens can vary significantly from their natural condition. Whether this approach might lead to misconceptions about the mechanical properties of ice has rarely been assessed. Furthermore, it is worth noting that even in some in-situ tests, the sea ice is taken out of the seawater for testing. To shed light on this issue, we have developed methods for testing floating ice specimens and compared the mechanical properties of ice while floating in water with properties measured in conventional laboratory experiments.

In this paper, we present our techniques for experimentation on floating ice tests in the laboratory. We also report results on the response of laboratory-grown, floating saline ice under low-stress cyclic compression. Moreover, to compare the mechanical properties measured for floating saline ice samples and those measured in more conventional experiments, we have also tested dry and isothermal saline ice. This paper summarizes findings earlier presented by Wei et al. (2020, 2022).

LABORATORY EXPERIMENTS

Ice preparation

The preparation and testing of the ice specimens were carried out in a cold room at Department of Mechanical Engineering, Aalto University. To prepare the saline ice specimens, tap water and aquarium salt were mixed in a water tank using a pump to form a saltwater solution with a salinity of 24 ppt. Then, several molds made of polyethylene, with dimensions of 600 mm × 300 mm × 110 mm (for uniaxial cyclic compression tests; Figure 1) were placed in the water tank. The molds could float on the water with only approximately 5 mm exposed. Seeding was started by lowering the laboratory temperature until the water cooled to -1.5°C. Freshwater at around 0°C was sprayed in a mist form above the water tank, met with cold air above, condensed into ice crystals, and fell onto the water surface until a thin layer of ice crystals was evenly distributed on the surface. Afterward, by maintaining the room temperature at -14°C for three days and -10°C for two days, an ice cover of approximately 11 cm was formed. Figures 2a and b show horizontal and vertical thin sections, respectively, under polarized light. The C-axes of the ice grains were found to lack a preferred orientation in the horizontal plane, with columnar structures clearly visible in the vertical thin section. The ice was identified of type S2 columnar.

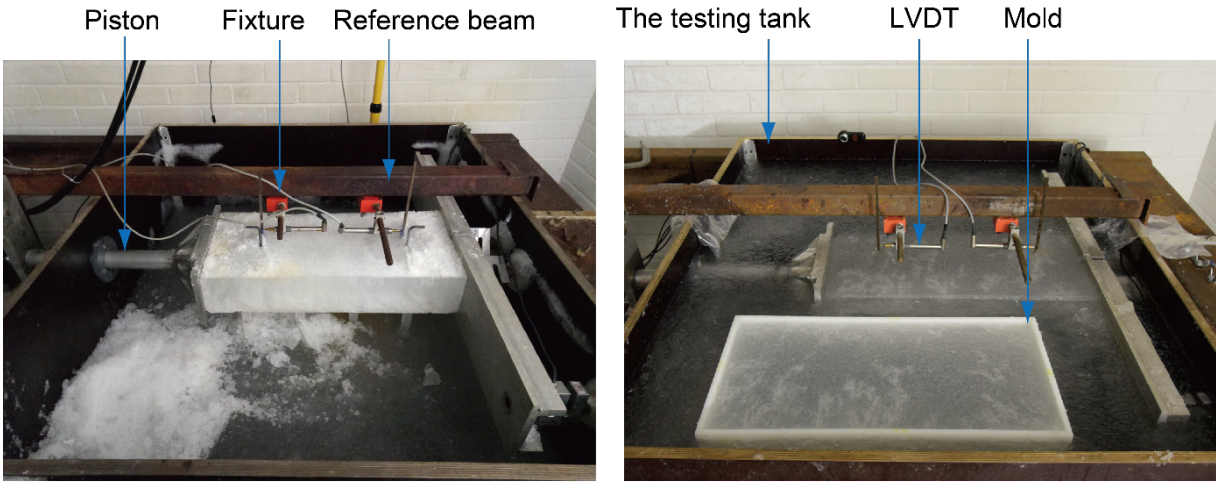

Figure 1. Specimen assemblies in the uniaxial cyclic compression experiments using (a) dry and (b) floating specimens.

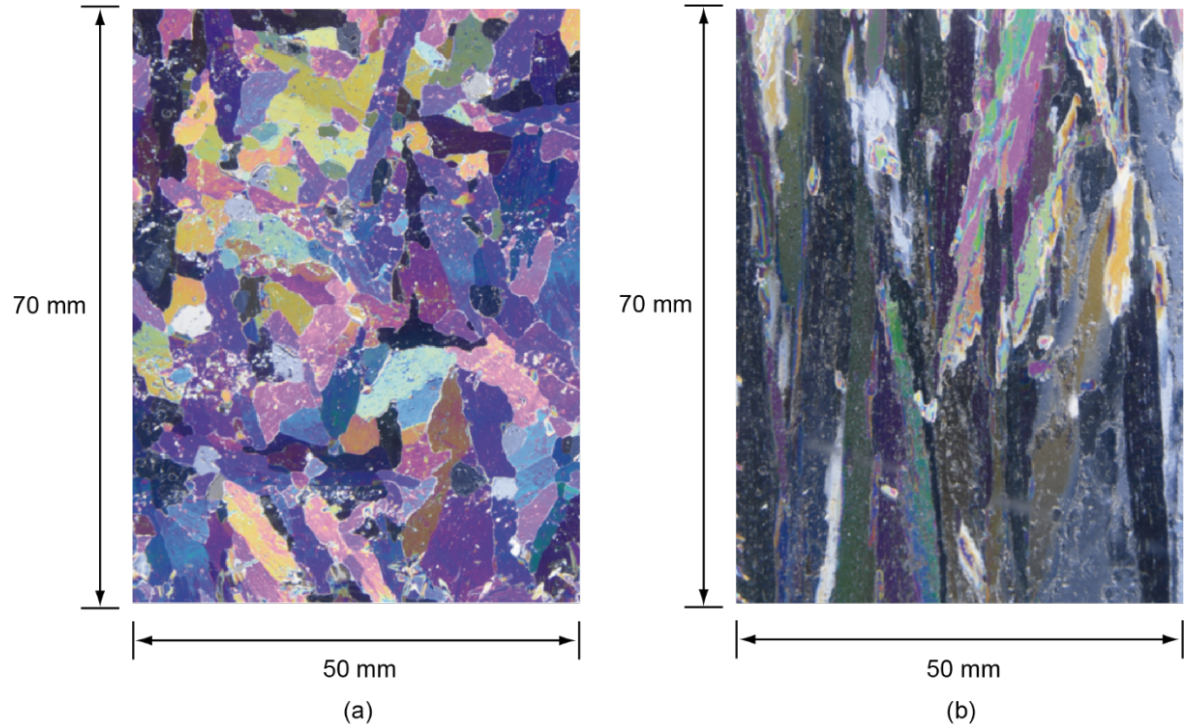

Figure 2. (a) Horizontal and (b) vertical thin sections of the ice.

Low-stress uniaxial cyclic compression tests

For the experiments with floating ice specimens (Figure 1b), before taking the sample out of the ice growth tank, a portion of saline water in the tank was first moved into the test tank (Figure 1). Then the specimens were taken out of the ice growing tank together with the molds, and their bottom surfaces were quickly trimmed to make them flat, after which they were rapidly transferred to the test tank. In the case of the dry ice experiments, the specimens needed to be stored at -2.5°C for 48 hours before testing, and the test tank was not filled with water during testing. Two vertical holes were then drilled into each specimen to allow for the insertion of two iron rods, frozen into the specimens with small quantity of freshwater at approximately

0°C. This allowed the use of linear variable differential transformers (LVDTs) for monitoring the displacements of the specimens along their axial directions, ultimately used to calculate the axial strains.

The primary objective of the cyclic loading experiments was to investigate the properties of the specimens obtained through the cyclic loading process at relatively low compressive stresses. The peak compressive stress ranged from 0.04 to 0.12 MPa. These stress levels were chosen to ensure that the specimens could produce detectable strains while avoiding significant damage or cracking. Each specimen was subjected to cyclic loads with frequencies of 1 Hz, 0.2 Hz, 0.1 Hz, 0.01 Hz, 0.002 Hz, and 0.001 Hz. In the loading waveform, the number of loading-unloading cycles with these frequencies were 10, 10, 10, 2, 1, and 1, respectively. For the floating and dry experiments, the ambient temperature was set at -10°C and -2.5°C, respectively. However, the average temperature of both dry and floating ice specimens was -2.5°C, which were measured using a three-channel temperature data logger. The temperature near the top surface, in the middle and near the bottom surface of the floating ice was approximately -3.0°C, -2.3°C and -2.2°C, respectively, in the testing process, without detectable change. For each experiment type, two specimens were used.

EXPERIMENTAL RESULTS

Figure 3 depicts typical stress-strain plots from specimens Dry-I and Floating-I. The stress-strain hysteresis loops are prominent, and their areas increase with decreasing loading frequency. Notably, at the same stress level, the floating ice exhibited higher levels of inelastic strain than the dry ice. This discrepancy became more apparent with decreasing loading frequency.

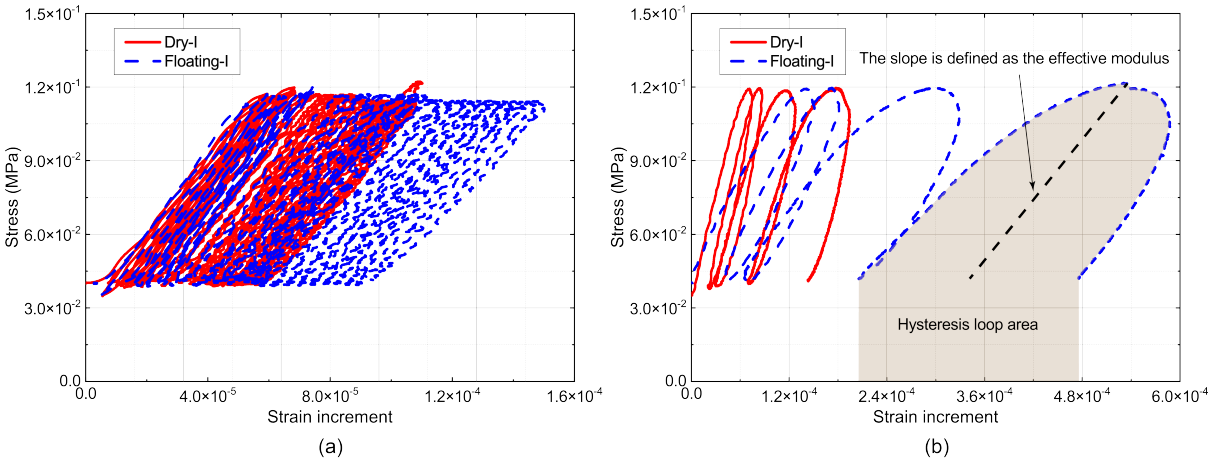

Figure 3. Comparison of representative stress-strain curves of the uniaxial cyclic compression specimens.

Figure 4a presents the effective moduli of the uniaxial compression specimens. The effective moduli were defined as demonstrated in Figure 3b. As the loading frequency increased, the effective moduli of both types of specimens increased accordingly. The effective moduli of the dry and floating ice specimens ranged from 1 to 2.2 GPa and from 0.4 to 1.8 GPa, respectively. Under a given loading frequency, the effective modulus of the floating ice was always smaller than that of the dry ice.

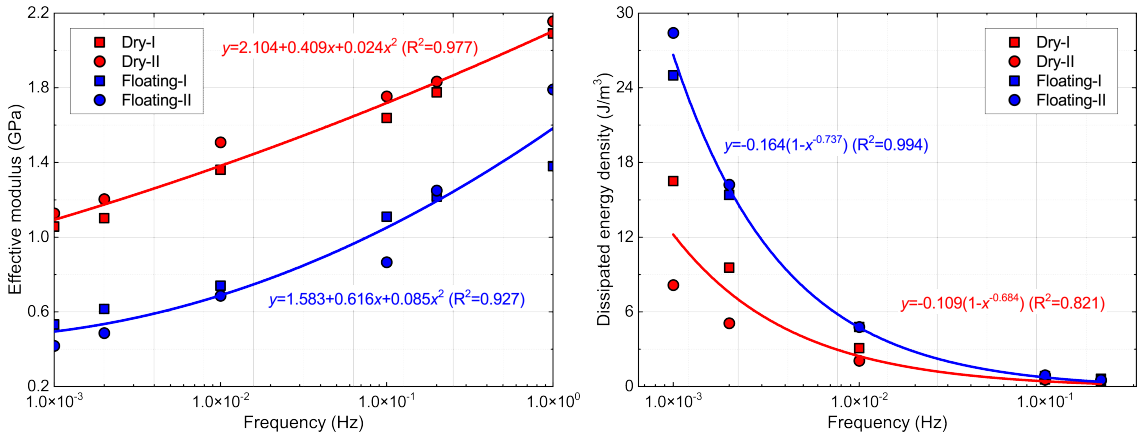

(a) (b)

Figure 4. (a) Effective moduli (GPa) of the dry and floating uniaxial compression specimens and (b) the energy density ($J \cdot m^{-3}$) dissipated in a representative loading-unloading cycle.

Figure 4b illustrates the energy density dissipated by the uniaxial compression specimens during a representative load-unload cycle. This quantity is equal to the area of the hysteresis loop as shown in Figure 3b. As the loading frequency increased, the dissipated energy density decreased. The relationship between the dissipated energy density and loading frequency roughly followed a power function. Under the same loading frequency, the energy density dissipated within one load-unload cycle for the floating ice was higher than for the dry ice. Further, Table 1 summarizes the energy dissipation rate for the uniaxial compression specimens in a representative loading-unloading cycle. This is equal to the consumed energy density divided by the maximum energy density input in this cycle. The energy dissipation rate increased with the loading-unloading period, T, regardless of whether the specimen was dry or floating. The energy dissipation rate increased from approximately 10% to 80%-90% when T increased from 5 s to 1000 s for both specimen types. Table 2 summarizes the internal friction determined from a representative loading-unloading cycle of each uniaxial compression specimen, calculated by dividing the hysteresis loop area by the area up to the stress peak. The difference in internal friction values between dry and floating ice specimens is negligible; both increasing from about 0.1 to 0.9 as the loading period increases from $T = 5$ s to $T = 1000$ s.

Table 1. The energy dissipation rate (%) determined in a relatively steady-state loading-unloading cycle

Specimen no.	T (s)				
	5	10	100	500	1000
Dry-I	9.23	14.1	45.7	75.2	88.4
Dry-II	11.1	12.9	37.1	60.8	80.5
Floating-I	11.8	15.5	44.2	76.1	89.6
Floating-II	11.3	17.4	39.4	69.8	87.7

Table 2. Internal friction determined in a relatively steady-state loading-unloading cycle.

Specimen no.	T (s)				
	5	10	100	500	1000
Dry-I	0.094	0.141	0.470	0.856	1.031
Dry-II	0.111	0.129	0.412	0.705	0.906
Floating-I	0.123	0.155	0.446	0.858	0.998
Floating-II	0.114	0.181	0.415	0.756	0.895

DISCUSSIONS

Analysis of the low-stress deformation behavior using a physics-based model

We analyzed the stress-strain plots from the uniaxial cyclic compression tests using a physics-based model developed in Cole (1995, 2004) and Cole and Durell (2001), in which anelasticity is considered to be due to dislocations and grain boundary relaxations while viscous straining results from basal dislocation glide. In the model, the elastic strain is determined by the elastic modulus and stress. The anelastic strain ε_a is calculated using (O'Connor et al., 2020):

$$\varepsilon_a = \sigma_0 J(t) + \int_0^t J(t-s)\frac{\delta\sigma}{\delta s}ds \tag{1}$$

where σ_0 is the stress at $t = 0$ s. $J(t)$ is a creep compliance, determined by

$$J(t) = \delta D_1^d \left\{1 - \frac{2}{\pi}\tan^{-1}[\exp(-\alpha^d \ln\frac{t}{\tau^d})]\right\} + \delta D_1^{gb}\left\{1 - \frac{2}{\pi}\tan^{-1}[\exp(-\alpha^{gb}\ln\frac{t}{\tau^{gb}})]\right\} \tag{2}$$

where δD_1^d is the dislocation relaxation strength and calculated using $\delta D_1^d (=\rho\Omega b^2 K^{-1})$. The meaning of the related parameters are summarized in Tables 3 and 4. Note that the parameters associated with grain boundary relaxation have similar physical meanings to those corresponding to lattice dislocations, but their values are different.

The viscous strain ε_v is expressed as

$$\varepsilon_v = \int_0^t \frac{\beta\rho\Omega^{1.5}b^2\sigma(t)}{B_0} e^{\left(-\frac{Q_{glide}}{kT^*}\right)}dt \tag{3}$$

with the parameters also explained in Tables 3 and 4, which also give their values measured in the experiments.

In this study, the determination of the elastic modulus primarily relied on the stress-strain relationship under high-frequency loading, while the dislocation density and grain boundary relaxation strength were determined from the non-elastic strain response. The dislocation density was the primary controlling factor that influenced the inelastic behavior. The calibrated parameter values are listed in Table 4, and some modeling results based on this model are presented in Figure 5. Figure 5 shows that the model could reproduce the strain response of the specimens under cyclic compression. Table 4 indicates that the average elastic modulus of the

dry specimens is approximately 21% higher than that of the floating specimens, while the average dislocation density of the dry specimens is only 38% of that of the floating ones.

Table 3. Fixed model parameters

Symbol	Meaning	Value
α^{d}	Peak broadening factor for dislocation relaxation	0.54
α^{gb}	Peak broadening factor for grain boundary relaxation	0.6
b	Burgers vector	4.52×10^{-10} (m)
B_0	Preexponential in dislocation drag term	1.205×10^{-9} (Pa)
k	Boltzmann constant	1.3806×10^{-23} (J/K)
K_d	Stress restoring term	0.07 (Pa)
Q_d	Activation energy for dislocation relaxation	0.55 (eV)
Q_{gb}	Activation energy for grain boundary relaxation	1.32 (eV)
β	Scaling factor	0.3
Ω	Orientation factor	$1/\pi$

Table 4. Calibrated model parameters for dry and floating specimens

Specimen no.	Elastic modulus E_0 (GPa)	Dislocation density ρ (m^{-2})	Strength of dislocation relaxation δD^{d} (Pa^{-1})	Strength of grain boundary relaxation δD^{gb} (Pa^{-1})
Dry-I	2.1–2.3	2.3×10^{9}–2.8×10^{9}	2.1×10^{-9}–2.6×10^{-9}	1.0×10^{-10}
Dry-II	2.0–2.2	1.5×10^{9}	1.4×10^{-9}	1.0×10^{-10}
Floating-I	1.4–2.0	4.6×10^{9}–5.3×10^{9}	4.3×10^{-9}–4.9×10^{-9}	3.0×10^{-10}
Floating-II	1.8–1.9	5.6×10^{9}	5.2×10^{-9}	1.0×10^{-10}

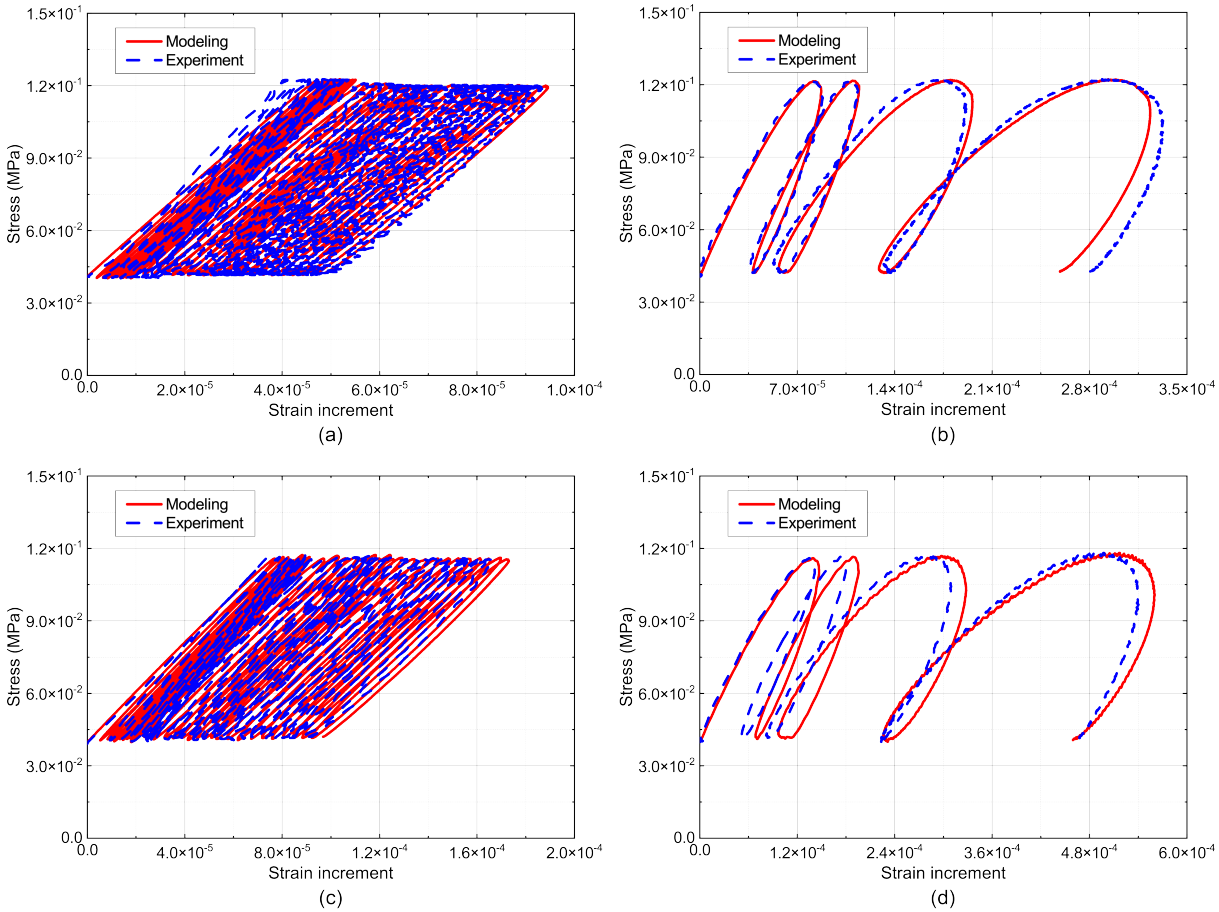

Figure 5. Comparison in the stress-strain plot of the uniaxial cyclic compression specimen between the physics-based modeling and the experiments. (a) and (b) plot the results for Specimen Dry-I; (c) and (d) give the results for Specimen Floating-I; (a) and (c) correspond to experiments with T = 1, 5, and 10 s; (b) and (d) correspond to experiments with T = 100, 500, and 1,000 s.

Interpretation of the mechanical behavior differences

The above results show clear differences in the mechanical behavior of the two types of ice specimens, as the floating ice has lower elastic modulus, lower flexural strength, and more pronounced rheological behavior than the dry ice. To explore the potential reasons for these differences, we carefully measured the densities and porosities of the two types of ice with the results showing that they are virtually equal for both specimen types: Densities of the dry and floating ice are about 904 kg·m^{-3}, and their total porosities are 0.121 and 0.125, respectively. Thus, we speculate that the differences in mechanical behavior differences may be attributed to the mechanism shown in Figure 6. When the ice was growing in the ice growth tank, some salt would be discharged from the ice and there was heat exchange between water and ice, resulting in many open brine drainage channels in the ice. However, after the ice was taken out of the tank and placed in a dry environment of -2.5°C, the water that remained in the fine brine drainage channels (such as due to the capillarity) might freeze. This process might not significantly reduce the porosity but might enhance the stiffness and reduce the rheological behavior of the ice. Observations of the textures, porosities and pore structures of the specimens before and after the cyclic loading could help to further confirm this. Making such observations close to the melting point, however, presents numerous technical challenges.

In the current stage of the work, it is evident from the analysis presented in Table 4 that the lower modulus and stronger viscoelastic response is associated with a substantially higher dislocation density in the floating vs. dry isothermal specimens as quantified by the constitutive model.

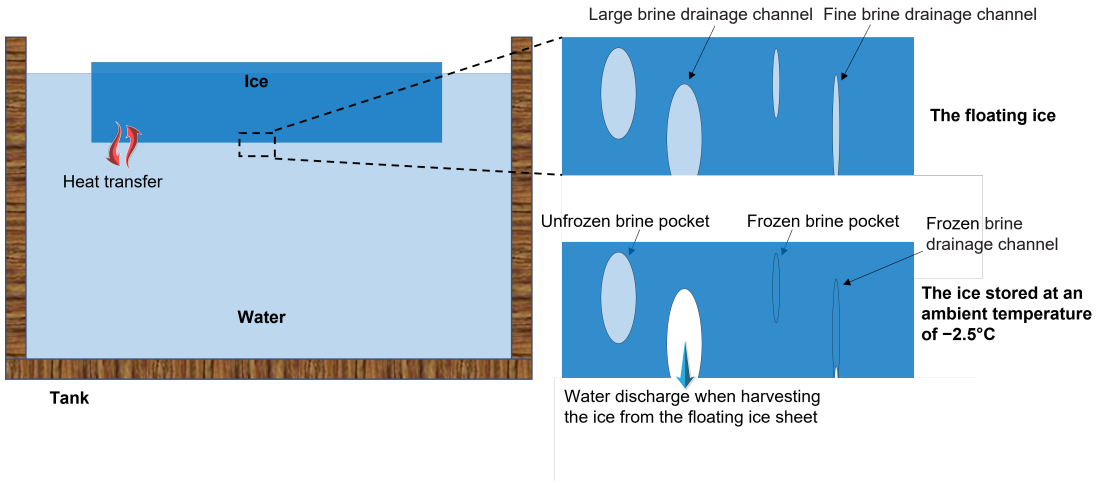

Figure 6. Schematic diagram of the inferred microstructure difference between the dry and floating ice

CONCLUSIONS

In this study, low-stress uniaxial compression tests were conducted on identically prepared saline ice specimens under two conditions: dry, isothermal and floating in saline water with a naturally occurring temperature gradient. The average temperatures, salinities, bulk densities and porosities of the specimens under both sets of conditions were approximately constant. However, the dry specimens showed ≈21% higher average elastic modulus and ≈62% lower average dislocation density than the floating specimens. Thus, the dry specimens were stiffer and behaved less rheological than the floating specimens. Therefore, attention should be paid when applying the mechanical properties measured from dry and isothermal ice specimens to in-situ sea ice-related problems. The above results make clear the importance of carrying out experiments on floating saline/sea ice specimens instead of exclusively examining ice behavior under dry isothermal conditions to understand and model sea ice behavior accurately.

ACKNOWLEDGEMENTS

The authors are grateful for financial support from the Academy of Finland (Ice Block Breakage: Experiments and Simulations, ICEBES; grant no. 309830).

REFERENCES

Cole, D.M., 1995. A model for the cyclic loading of saline ice subjected to cyclic loading. *Philosophical Magazine A*, 72(1), 231-248.

Cole, D.M., 2004. A dislocation-based model for creep recovery in ice. *Philosophical Magazine*, 84(30), 3217-3234.

Cole, D.M., & Durell, G.D., 2001. A dislocation-based analysis of strain history effects in ice. *Philosophical Magazine A*, 81(7), 1849-1872.

Feltham, D.L., 2008. Sea ice rheology. *Annual Review of Fluid Mechanics*, 40(1), 91-112.

Iliescu, D., Murdza, A., Schulson, E.M., & Renshaw, C.E., 2017. Strengthening ice through cyclic loading. *Journal of Glaciology*, 63(240), 663-669.

Langhorne, P.J., Squire, V.A., Fox, C., & Haskell, T.G., 1998. Break-up of sea ice by ocean waves. *Annals of Glaciology*, 27, 438-442.

Murdza, A., Marchenko, A., Schulson, E.M., & Renshaw, C.E., 2020a. Cyclic strengthening of lake ice. *Journal of Glaciology*, 67(261), 182-185.

Murdza, A., Schulson, E.M., & Renshaw, C.E., 2020b. Strengthening of columnar-grained freshwater ice through cyclic flexural loading. *Journal of Glaciology*, 66(258), 556-566.

Murdza, A., Schulson, E.M., & Renshaw, C.E., 2021. Behavior of saline ice under cyclic flexural loading. *The Cryosphere*, 15(5), 2415-2428.

Murdza, A., Schulson, E.M., & Renshaw, C.E., 2022. Relaxation of flexure-induced strengthening of ice. *Geophysical Research Letters*, 49(4), e2021GL096559.

O'Connor, D., West, B., Haehnel, R., Asenath-Smith, E., & Cole, D., 2020. A viscoelastic integral formulation and numerical implementation of an isotropic constitutive model of saline ice. *Cold Regions Science and Technology*, 171, 102983.

Squire, V.A. 2020. Ocean wave interactions with sea ice: A reappraisal. *Annual Review of Fluid Mechanics*, 52(1), 37-60.

Wei, M., Polojärvi, A., Cole, D.M., & Prasanna, M., 2020. Strain response and energy dissipation of floating saline ice under cyclic compressive stress. *The Cryosphere*, 14(9), 2849-2867.

Wei, M., Prasanna, M., Cole, D.M., & Polojärvi, A., 2022. Response of dry and floating saline ice to cyclic compression. *Geophysical Research Letters*, 49, e2022GL099457.